PNAS RESEARCH ARTICLE | NEUROSCIENCE

Active forgetting requires Sickie function in a dedicated dopamine circuit in *Drosophila*

Xiaofan Zhang[a], John Martin Sabandal[a], George Tsaprailis[b], and Ronald L. Davis[a,c,1]

Edited by Ann-Shyn Chiang, National Tsing Hua University, Hsinchu, Taiwan; received March 9, 2022; accepted August 4, 2022 by Editorial Board Member Liqun Luo

Forgetting is an essential component of the brain's memory management system, providing a balance to memory formation processes by removing unused or unwanted memories, or by suppressing their expression. However, the molecular, cellular, and circuit mechanisms underlying forgetting are poorly understood. Here we show that the memory suppressor gene, *sickie*, functions in a single dopamine neuron (DAn) by supporting the process of active forgetting in *Drosophila*. RNAi knockdown (KD) of *sickie* impairs forgetting by reducing the Ca^{2+} influx and DA release from the DAn that promotes forgetting. Coimmunoprecipitation/mass spectrometry analyses identified cytoskeletal and presynaptic active zone (AZ) proteins as candidates that physically interact with Sickie, and a focused RNAi screen of the candidates showed that Bruchpilot (Brp)—a presynaptic AZ protein that regulates calcium channel clustering and neurotransmitter release—impairs active forgetting like *sickie* KD. In addition, overexpression of *brp* rescued the impaired forgetting of *sickie* KD, providing evidence that they function in the same process. Moreover, we show that *sickie* KD in the DAn reduces the abundance and size of AZ markers but increases their number, suggesting that Sickie controls DAn activity for forgetting by modulating the presynaptic AZ structure. Our results identify a molecular and circuit mechanism for normal levels of active forgetting and reveal a surprising role of Sickie in maintaining presynaptic AZ structure for neurotransmitter release.

active forgetting | dopamine | *Drosophila* | Sickie | Bruchpilot

Forgetting, the flip side of memory acquisition and consolidation, is an essential component of the brain's memory management system that provides a balance to memory formation processes by removing unused or unwanted memories, or by suppressing their expression (1, 2). However, the molecular, cellular, and circuit mechanisms underlying forgetting are poorly understood.

Previous studies showed that dopamine (DA) and its downstream signaling molecules in postsynaptic neurons are essential for active forgetting and transient forgetting (3–7) in *Drosophila*. Small subsets of DA neurons (DAn) within the PPL1 cluster of 12 DAn that innervate the *Drosophila* mushroom body neurons (MBn) mediate forgetting. Blocking the synaptic output from these DAn after learning inhibits forgetting, whereas stimulating the DAn increases forgetting (3). Moreover, external factors and internal states, such as locomotor activity, stress, and arousal increase the ongoing activity of these DAn and accelerate forgetting. Conversely, sleep or rest after learning, which decreases the ongoing activity of these DAn, inhibits forgetting (4). This DA-based forgetting is mediated by a DA receptor, DAMB, expressed on the postsynaptic MBn, and requires a downstream signaling pathway involving Scribble, Rac1, and Cofilin for actin remolding (5–7).

A large RNA interference (RNAi) screen of ∼3,500 genes identified *sickie* as a memory suppressor genes in *Drosophila* (8). It was classed as such because knockdown (KD) of *sickie* led to increased memory expression. Sickie was initially found to be required for the nuclear translocation of Relish for normal innate immune responses using cultured *Drosophila* S2 cells (9). Its homologs, NAV2 in humans and Unc53 in *Caenorhabditis elegans*, were reported to control neurite outgrowth and the anteroposterior directional guidance of some migratory cells (10–12). Other studies also suggested that NAV2 is an oncogene whose expression level is closely related to several human tumors (13–15). A recent study found that Sickie regulates F-actin–mediated axon growth of *Drosophila* MBn (16). However, *sickie*'s role in learning and memory was not explored, and its mechanism for memory suppression was unknown.

Here, we show that *sickie* is required in a single DAn for active forgetting, but not for memory acquisition or consolidation. *Sickie* KD impairs forgetting by reducing the ongoing activity of DAn. Coimmunoprecipitation and mass spectrometry (co-IP/MS) experiments identify presynaptic active zone (AZ) proteins as the top candidates that

Significance

Forgetting, the flip side of memory acquisition and consolidation, provides a balance to memory formation processes by removing unused or unwanted memories, or by suppressing their expression. However, the mechanisms underlying forgetting are poorly understood. Here, we identify a molecular and circuit mechanism for active forgetting. Reducing Sickie levels in a single dopamine neuron (DAn) impairs active forgetting by decreasing the ongoing DAn activity. Sickie regulates forgetting by interacting with the presynaptic active zone (AZ) protein Bruchpilot, and altering the structure of the DAn AZ. We propose that Sickie maintains the integrity and function of the DAn AZ by interacting with presynaptic AZ proteins, including Bruchpilot, allowing for the normal ongoing release of DA for active forgetting.

Author affiliations: [a]Department of Neuroscience, Scripps Research Institute Florida, Jupiter, FL 33458; [b]Proteomics Core, UF Scripps Biomedical, Jupiter, FL 33458; and [c]Department of Neuroscience, UF Scripps Biomedical, Jupiter, FL 33458

Author contributions: X.Z. and R.L.D. designed research; X.Z. and J.M.S. performed research; G.T. contributed new reagents/analytic tools; X.Z. and J.M.S. analyzed data; and X.Z. and R.L.D. wrote the paper.

The authors declare no competing interest.

This article is a PNAS Direct Submission. A.-S.C. is a guest editor invited by the Editorial Board.

[1]To whom correspondence may be addressed. Email: ronalddavis@ufl.edu.

This article contains supporting information online at http://www.pnas.org/lookup/suppl/doi:10.1073/pnas.2204229119/-/DCSupplemental.

Published September 12, 2022.

interact with Sickie. An RNAi screen of the top candidates along with additional experiments reveal that Sickie interacts physically and genetically with Bruchpilot (Brp) to mediate forgetting through the DAn. Moreover, we show that *sickie* KD alters the structure of the presynaptic AZ. Taken together, our results suggest a model whereby Sickie maintains the normal structure and function of presynaptic AZ of a single DAn for DA-based forgetting, through its interaction with presynaptic AZ protein Brp and regulating neurotransmitter release.

Results

***Sickie* Is Required in a Single DAn for Memory Suppression.** In a large RNAi screen for effects on 3-h aversive olfactory memory expression in *Drosophila*, we identified *sickie* as a memory-suppressor gene whose KD in the *TH-gal4* labeled PPL1 cluster DAn resulted in 3-h memory enhancement (8). There are ∼12 DAn in the PPL1 cluster (17) and to identify which specific DAn require *sickie*'s function, we performed a behavioral screen using a collection of *gal4* drivers that cover the subpopulations of PPL1 DAn (Fig. 1*A*). We found that 3-h memory was significantly enhanced only when *sickie* RNAi was expressed in neurons that include MP1 (PPL1γ1pedc) DAn (with drivers *TH*, *c150*, and *c061*: *TH* labels all PPL1 DAn; *c150* labels MP1, MV1/PPL1-γ2α′1 and V1/PPL1-α′2α2; *c061* only labels MP1 DAn), compared to the Control (the parental line containing the docking site used for insertion of the RNAis). Expressing *sickie* RNAi in other PPL1 subpopulations (MV1, V1, PPL1-α′3, and PPL1-α3) had no significant effect on 3-h memory (Fig. 1*A*). We found no difference in odor or shock avoidance behavior of the *sickie* KD flies that could account for the enhanced memory performance (*SI Appendix*, Fig. S1*A*).

The observed memory enhancement phenotype was reproduced using *c061-Gal4;MBgal80* driving another two *sickie* RNAis (Fig. 1 *B* and *C*) (TRIP RNAi^{54037} and RNAi^{53315}), which target different sequences in the *sickie* RNA transcripts (*SI Appendix*, Fig. S1*D*). We focused further experimentation on TRIP RNAi^{54037}, which showed more efficient KD measured by Western blotting (73% vs. 35% efficiency compared to RNAi^{107037}) (Fig. 1*F* and *SI Appendix*, Fig. S2). Although *c061-Gal4;MBgal80* labels MP1 DAn, it also labels some non-DA neurons (6). To confirm that the memory enhancement is due to *sickie*'s function in MP1 DAn, we took advantage of a *split-gal4 MB320C* that specifically labels MP1 DAn, a single DAn (one per hemisphere) that innervates the heel region of the MB lobe (Fig. 1*E*). Expressing two *sickie* RNAis in MP1 DAn with *MB320C split-gal4* confirmed that *sickie* KD in MP1 DAn significantly enhanced 3-h memory (Fig. 1*D* and *SI Appendix*, Fig. S1*C*). *Sickie* RNAi expression in MP1 DAn (*c061-Gal4;MBgal80* and *MB320C split-gal4*) enhanced memory compared to both *gal4*-only and *UAS*-only control flies (*SI Appendix*, Fig. S1*B*), eliminating potential chromatin position effects on the transgenes used. The *sickie* RNAi lines (KK and TRIP lines) also showed no significant difference when compared with their parental lines (*SI Appendix*, Fig. S7*E*), supporting the lack of chromatin position effects at the docking site for the RNAi transgenes. We also found that overexpression of wild-type *sickie* (*UAS-sickie*) or a functional mCherry tagged-wild-type *sickie* (*UAS-mCherry-sickie*) had no effect alone on 3-h memory but rescued the *sickie* KD induced 3-h memory enhancement (*SI Appendix*, Fig. S3). These results suggest that wild-type levels of *sickie* are not limiting for memory performance.

We then studied the developmental time for *sickie*'s role in olfactory memory. To do this, we employed the TARGET system (18) to temporally control *sickie* RNAi expression in MP1 DAn by manipulating the incubation temperatures. The expression of *sickie* RNAi is inhibited when the flies are kept at 18 °C (restrictive temperature) but induced when flies are kept at 30 °C (permissive temperature). We found that *sickie* KD in MP1 DAn during adulthood, but not during earlier developmental periods, was sufficient to enhance 3-h memory (Fig. 1*G*).

***Sickie* KD Does Not Alter Memory Acquisition.** DAn have been shown to be involved in memory acquisition, consolidation, and forgetting (3, 4, 7, 19–22), so the enhancement of 3-h memory due to *sickie* KD could be due to a role in any of these processes. We first studied *sickie*'s role in memory acquisition. We varied the number of electric shocks the flies receive during training and tested the performance immediately after training (3-min memory), using flies expressing *sickie* RNAi in MP1 DAn with *MB320C-split-gal4*. We found that there was no significant difference between *sickie* KD and control flies (Fig. 2*A*). We also varied the shock intensity during training and tested performance immediately after training. Again, there was no significant difference between *sickie* KD and control flies (Fig. 2*B*). We also tested the memory acquisition by varying the shock number and intensity using a second *sickie* RNAi and observed the same results (*SI Appendix*, Fig. S4). Thus, memory acquisition experiments are not consistent with *sickie* limiting this process.

Electric shock is thought to activate all PPL1 DAn during training as the unconditioned stimulus (US) (17), so that the unaltered acquisition observed with *sickie* KD specifically in MP1 DAn could be attributed to a compensatory response from other PPL1 DAn. To test for this possibility, we limited the US to MP1 DAn by substituting electric shock with thermal activation of MP1 DAn, with expression of TrpA1 at an elevated temperature during training. TrpA1 activation of MP1 DAn during training induced significantly higher 3-min and 3-h memory compared to control flies without TrpA1 activation. This is consistent with previous studies showing that MP1 DAn is required for memory acquisition (23, 24). Notably, we found that 3-h memory but not 3-min memory was significantly enhanced in the flies expressing *sickie* RNAi (Fig. 2*C*). These results further argue that *sickie*'s role in 3-h memory suppression does not occur by inhibiting memory acquisition.

***Sickie* KD Enhances Labile but Not Consolidated Memory.** Next, we tested *sickie*'s role in memory consolidation. The enhanced 3-h memory in *sickie* KD flies may be due to increased labile memory or consolidated memory, or both. To probe this, we first examined memory retention by testing performance at different times after training (3 min−24 h). We found that *sickie* KD in MP1 DAn significantly increased 3- and 6-h memory, but not 3-min, 1-h, or 24-h memory (Fig. 2*D*). Because memory remaining at 24 h after training is primarily consolidated memory (25), this result suggests that *sickie* KD does not alter memory consolidation.

Consolidated memory that forms after our single cycle training procedures is termed anesthesia-resistant memory (ARM), due to its insensitivity to cold shock. In contrast, memory eliminated by cold shock is termed anesthesia-sensitive memory (ASM). Flies were subjected to a 2 min cold shock at 2 h after training to eliminate the labile ASM and subsequently tested at 3 h to measure ARM. If *sickie* KD altered ARM consolidation, one would observe an enhancement in 3-h memory even in flies subjected to cold shock. However, we found that cold shock abolished the 3-h memory enhancement in *sickie* KD

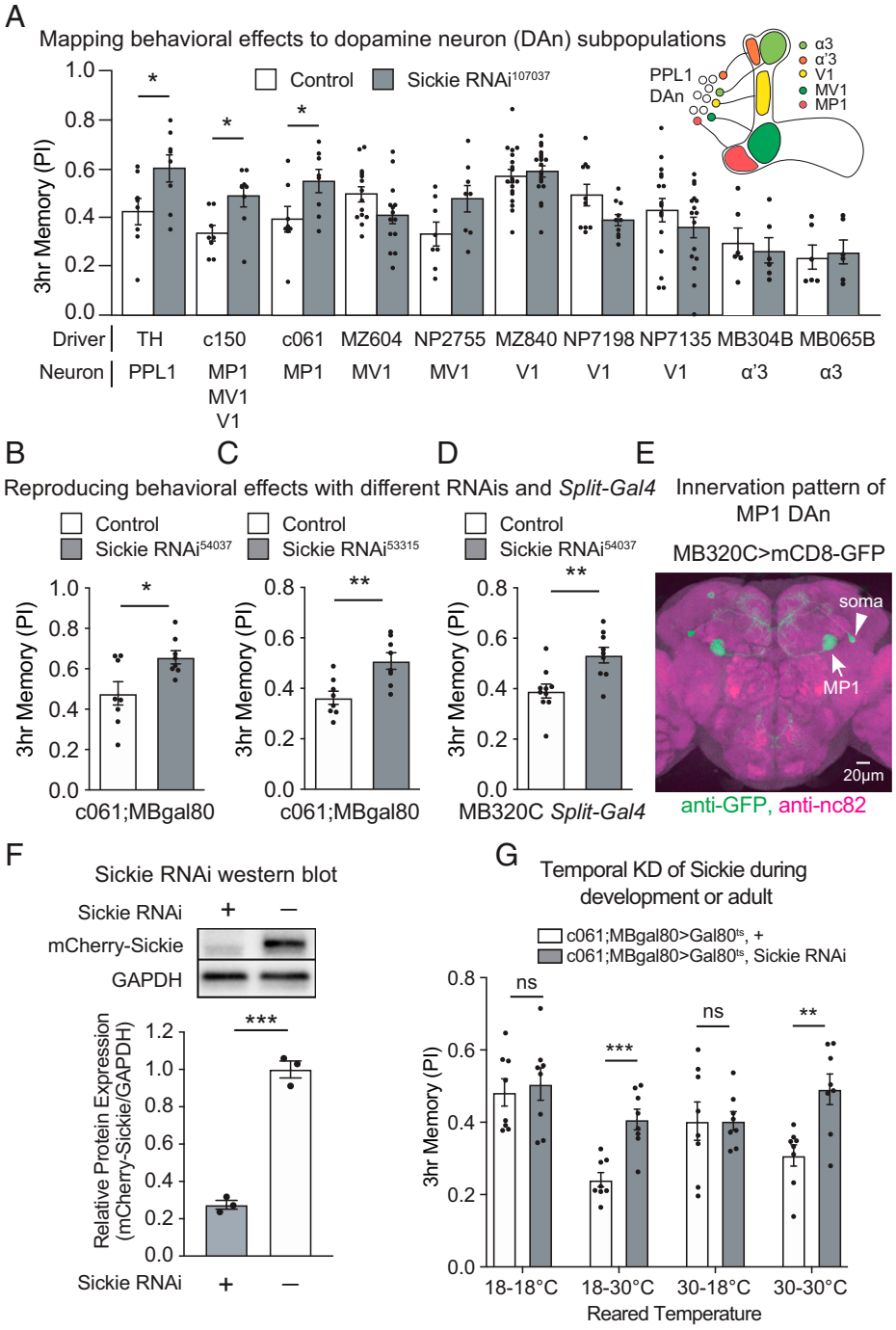

Fig. 1. *Sickie* is required in MP1 (PPL1γ1pedc) DAn, a subset of PPL1 DAn, for memory suppression. (*A*) KD of *sickie* in MP1 DAn (*TH-gal4*, *c150-Gal4*, and *c061-Gal4;MBgal80*) enhanced 3-h memory scores. The schematic illustrates the 12 DAn in each PPL1 cluster that innervate distinct segments of the MBn neuropil. Control: *Gal4*>+. *sickie* RNAi^{107037}: *Gal4* > *UAS-Dcr2, UAS-sickie-RNAi*^{107037}. See *Materials and Methods* for the specific definition of "Control" for this and subsequent figures. Student's *t* test, **P* < 0.05; *n* = 6 to 19; mean ± SEM. (*B* and *C*) KD of *sickie* in MP1 DAn with TRIP RNAi^{54037} and RNAi^{53315} increased 3-h memory scores. (*B*) Control: *c061-Gal4;MBgal80*>+. *sickie* RNAi^{54037}: *c061-Gal4; MBgal80* > *UAS-sickie-RNAi*^{54037}. (*C*) Control: *c061-Gal4;MBgal80* > *UAS-Dcr2*, +. *sickie* RNAi^{53315}: *c061-Gal4; MBgal80* > *UAS-Dcr2, UAS-sickie-RNAi*^{53315}. Student's *t* test, **P* < 0.05, ***P* < 0.01; *n* = 8; mean ± SEM. (*D*) KD of *sickie* in MP1 DAn with *MB320C-Split-gal4* increased 3-h memory scores. Control: *MB320C*>+. *sickie* RNAi^{54037}: *MB320C* > *UAS-sickie-RNAi*^{54037}. Student's *t* test, ***P* < 0.01; *n* = 9 to 10; mean ± SEM. (*E*) Innervation pattern of MP1 DAn in the brain driven by *MB320C-Split-gal4* > *UAS-mCD8-GFP*. Arrow: MP1 region; arrowhead: soma of MP1 DAn. (*F*) Western blot of fly head lysates showed that pan-neuronal KD of *sickie* significantly reduced mCherry tagged Sickie protein (see *SI Appendix*, Fig. S2 for full Western blot image and Western blot of *sickie* RNAi^{107037}). *sickie* RNAi +: *nSyb* > *UAS-sickie-RNAi*^{54037}, *UAS-mCherry-sickie*^{WT}. *sickie* RNAi –: *nSyb*>+, *UAS-mCherry-sickie*^{WT}. Mann–Whitney *U* test, ****P* < 0.001; *n* = 3; mean ± SEM. (*G*) KD of *sickie* only during adulthood using the TARGET system was sufficient to increase 3-h memory scores. The *Gal80*^{ts} transgene inhibits *Gal4* activity at 18 °C but not at 30 °C. Student's *t* test, ***P* < 0.01, ****P* < 0.001; *n* = 8; mean ± SEM.

flies (Fig. 2*E*), indicating that the increased 3-h memory in *sickie* KD flies is due to increase of labile memory. We also found no significant difference in 24-h memory performance in *sickie* KD flies subjected to 5× massed training (Fig. 2*F*). The memory remaining at 24 h after 5× massed training is also principally ARM. This observation further supports the conclusion that *sickie* KD does not enhance memory consolidation. Rather, the memory enhancement in *sickie* KD flies increases labile memory.

MP1 DAn Bidirectionally Regulate Forgetting, and *sickie* Is Involved in MP1 DAn for Forgetting. Next, we tested whether *sickie* is involved in MP1 DAn for DA-based forgetting. Our prior studies have shown that activation of DAn after training accelerates forgetting, while blocking DAn after training inhibits it (3, 7). We reasoned that if *sickie* mediates forgetting through a function in MP1 DAn, then *sickie* KD in MP1 DAn and blocking the activity of MP1 DAn should produce similar results on memory performance. Our prior study using *c061-Gal4* to drive *shi*^{ts1} at 32 °C to block MP1 DAn after training failed to enhance 3-h memory (3). However, high-temperature incubation caused a marked reduction of memory in control genotypes (*UAS-shi*^{ts1} and *c061-Gal4* flies), whereas no reduction of memory was observed in the experimental group (*c061-Gal4* > *UAS-shi*^{ts1}). These results suggest that the expected memory enhancement was masked by a heat stress-induced memory loss in the experimental group. This led us to choose the optogenetics tool GtACR1, an anion channelrhodopsin that inhibits neuronal activity upon exposure to green light (26), to block the MP1 DAn with the more specific *split gal4*, *MB320C*. We found that blocking MP1

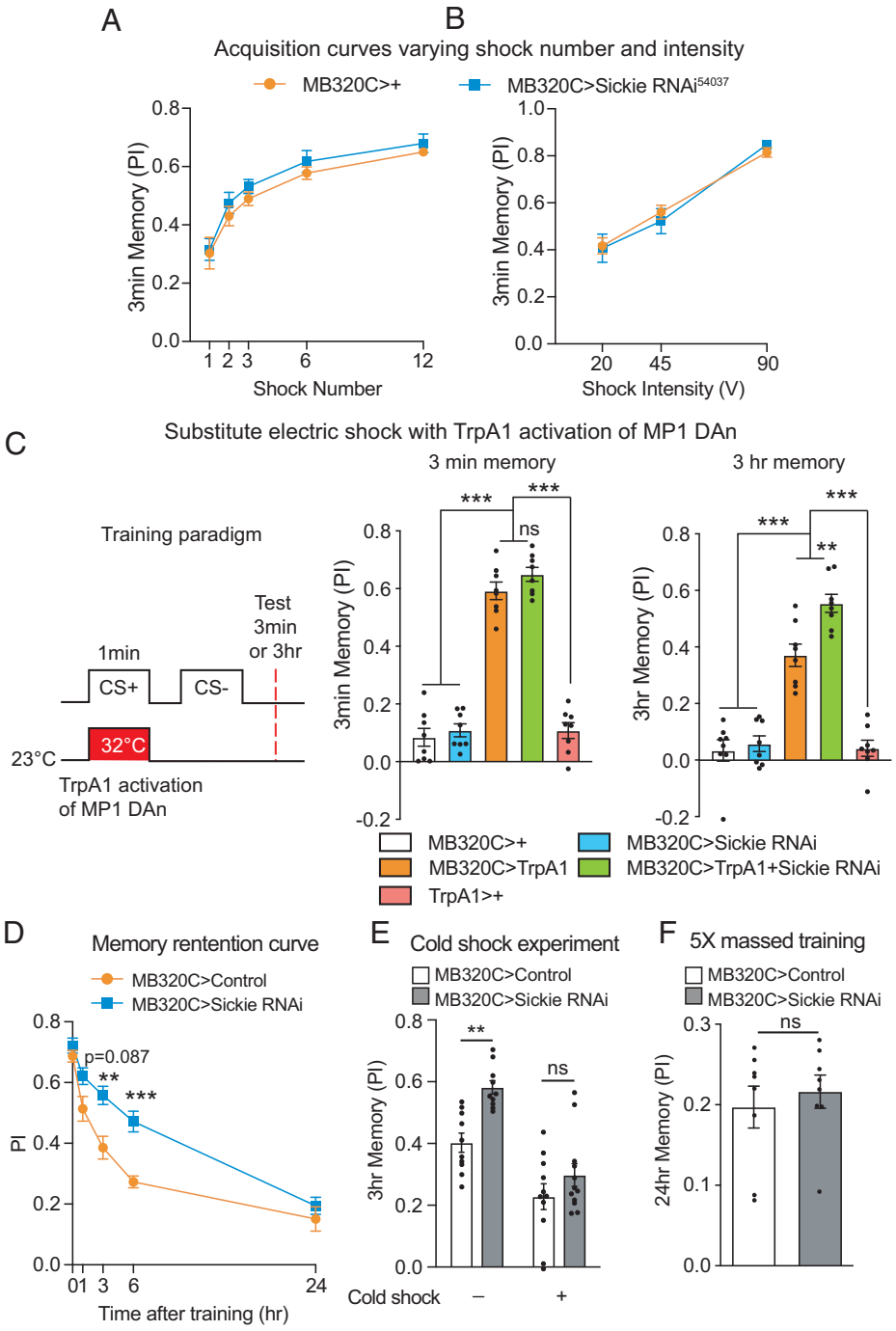

Fig. 2. *Sickie* KD in MP1 DAn does not alter memory acquisition and consolidation, but enhances labile memory. (*A*) KD of *sickie* in MP1 DAn did not alter memory acquisition with a variable number of shock pulses. Student's *t* test; $n = 6$; mean ± SEM. (*B*) KD of *sickie* in MP1 DAn did not alter memory acquisition using altered shock intensity. Student's *t* test; $n = 6$; mean ± SEM. (*C*) Substituting electric shock with TrpA1 activation of MP1 DAn during training and knocking down *sickie* in MP1 DAn did not alter 3-min memory (*Center*). Rather, it significantly increased 3-h memory (*Right*). Flies were raised and kept in 23 °C before training. During training, flies were transferred to prewarmed training tube in 32 °C and received the CS^+ odor for 1 min. The flies were transferred back to 23 °C to receive another 1 min of CS^- odor. After training, flies were kept in 23 °C and tested for 3-min or 3-h memory (*Left*). One-way ANOVA with Tukey's multiple comparisons test. $^{**}P < 0.01$, $^{***}P < 0.001$; $n = 8$; mean ± SEM. (*D*) KD of *sickie* in MP1 DAn increased memory retention at 3 and 6 h, but not at 3 min, 1 h, and 24 h after training. Two-way ANOVA with Bonferroni's multiple comparisons test. $^{**}P < 0.01$, $^{***}P < 0.001$; $n = 8$; mean ± SEM. (*E*) KD of *sickie* in MP1 DAn did not alter ARM. In the cold shock group (+), flies received 2 min of cold shock at 2 h after training to eliminate ASM. Two-way ANOVA with Bonferroni's multiple comparisons test. $^{**}P < 0.01$, ns, not significant; $n = 10$ to 12; mean ± SEM. (*F*) KD of *sickie* in MP1 DAn did not alter memory consolidation produced by massed training. Student's *t* test. ns, not significant; $n = 8$; mean ± SEM.

DAn with GtACR1 expression and green light exposure in experimental flies (*MB320C > UAS-GtACR1*) between training and testing significantly enhanced 3-h memory, while green light exposure had no effect on control fly (*MB320C>+ or UAS-GtACR1>+*) performance (Fig. 3*A*). The memory enhancement observed with experimental flies is not due to an effect on memory retrieval, since blocking MP1 DAn for 5 min immediately before testing was without effect (Fig. 3*B*). This conclusion was reinforced by results showing that channel activation from 0 to 160 or 0 to 175 min after training is sufficient to enhance memory (*SI Appendix*, Fig. S5*A*). Together, these data indicate that blocking MP1 DAn is sufficient to inhibit forgetting.

These blocking data strongly suggested that the 3-h memory enhancement induced by *sickie* KD occurs from its function in MP1 DAn for forgetting. To test this hypothesis, we asked whether *sickie* KD rescues forgetting caused by the activation of MP1 DAn. We found that activation of MP1 DAn after training with TrpA1 at 25 °C significantly reduced 3-h memory (Fig. 3*C*) (*MB320C> UAS-TrpA1*, 23 °C vs. 25 °C). Control genotypes without the *gal4* or *UAS-TrpA1* transgenes did not show the forgetting phenotype at 25 °C (*SI Appendix*, Fig. S5*B*) as observed in experimental groups (Fig. 3*C*). This is consistent with previous findings that activation of MP1 DAn after training induces forgetting (3). These data, together with the GtACR1 blocking data, demonstrate that MP1 DAn alone is sufficient to bidirectionally regulate forgetting. More importantly, we found that *sickie* KD in MP1 DAn fully rescued mild and moderate TrpA1 activation induced forgetting (Fig. 3*C* and *SI Appendix*, Fig. S5*C*), and partially rescued strong TrpA1 activation induced forgetting (*SI Appendix*, Fig. S5*D*).

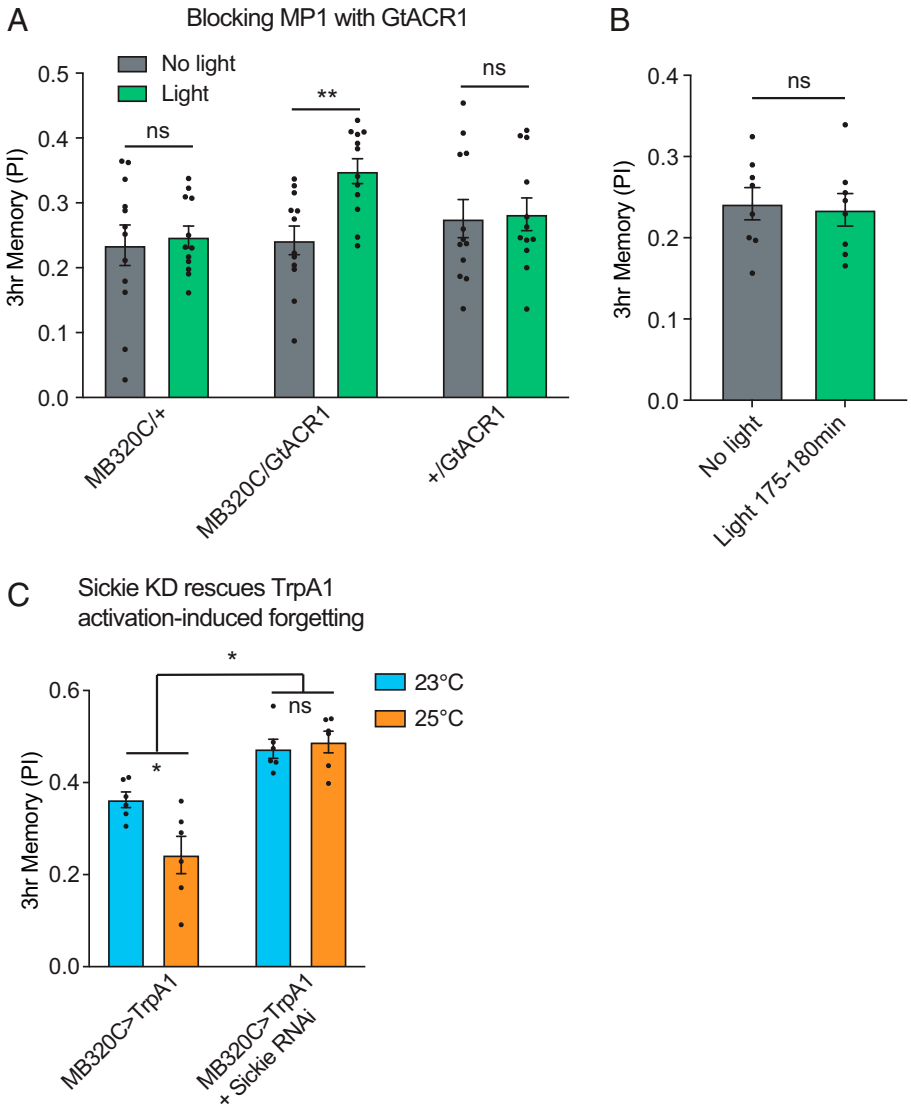

Fig. 3. MP1 DAn bidirectionally regulates forgetting. (*A*) Blocking MP1 DAn by activating GtACR1 after training impaired forgetting. Two-way ANOVA with Bonferroni's multiple comparisons test. $^{**}P < 0.01$, ns, not significant; $n = 12$; mean ± SEM. (*B*) Blocking MP1 DAn by activating GtACR1 for 5 min before testing did not alter 3-h memory performance. Student's *t* test. ns, not significant; $n = 8$; mean ± SEM. (*C*) Activation of MP1 DAn with mild TrpA1 activation after training induced forgetting (23 °C vs. 25 °C in the *MB320C > TrpA1* group), and *sickie* KD in MP1 DAn rescued TrpA1 activation-induced forgetting. Two-way ANOVA with Bonferroni's multiple comparisons test. $^{*}P < 0.05$, ns, not significant; $n = 6$; mean ± SEM.

These results, along with those described below (Fig. 4 *C* and *D*), indicate that *sickie* functions in MP1 DAn for forgetting.

***Sickie* Regulates Ongoing DAn Activity in MP1 DAn for Forgetting.** How does *sickie* function in MP1 DAn to modulate forgetting? The rescue of TrpA1-induced forgetting with *sickie* KD suggests that it suppresses MP1 DAn activity, opposing TrpA1-induced activity. Since DAn are known to mediate the US of electric shock during associative learning, we first asked whether *sickie* KD suppresses MP1 DAn activity produced by electric shock. Flies were mounted under a confocal microscope for in vivo functional imaging and electric shock pulses were applied that mimics the conditions used for behavioral training. We observed a clear peak with each shock pulse of intracellular Ca^{2+} increase with the sensor GCaMP6f (Fig. 4*A*) and DA release with the DA sensor GRABDA2m (Fig. 4*B*) in the MP1 region. However, we failed to observe a significant difference in Ca^{2+} response (Fig. 4*A*) or DA release (Fig. 4*B*) between *sickie* KD and control flies, estimated by the area under the response profile during the delivery of electric shock pulses (from 30 to 90 s). These results indicate that *sickie* KD does not alter MP1 DAn activity produced upon stimulation by electric shock. Because MP1 DAn activity during training is required for memory acquisition, these results are also consistent with our finding that *sickie* KD does not alter memory acquisition.

Our behavioral data obtained upon blocking MP1 DAn ongoing activity indicate that this treatment impairs forgetting (Fig. 3*A*), which is consistent with prior studies (3, 4). So, we asked whether *sickie* KD impairs forgetting by suppressing the ongoing activity of MP1 DAn. We expressed the Ca^{2+} sensor GCaMP6f or the DA sensor GRABDA2m in MP1 DAn and monitored the ongoing intracellular Ca^{2+} responses and DA release in MP1 using the same in vivo functional imaging procedures as above, but without delivering electric shock pulses or other stimuli. We found under these conditions that *sickie* KD in MP1 DAn resulted in a significant reduction of the ongoing Ca^{2+} responses (Fig. 4*C*) and DA release (Fig. 4*D*) when compared to the control flies. Our previous study showed that forward or backward conditioning failed to alter the ongoing Ca^{2+} activity at 15 to 25 min posttraining observed in DAn of untrained flies (3). Consistent with this, we failed to observe any difference in activity using control flies across three 15-min time windows after conditioning (*SI Appendix*, Fig. S5*E*). In contrast, we observed a significant reduction of the ongoing Ca^{2+} activity after training in the *sickie* KD group (*SI Appendix*, Fig. S5*E*). These data, together with the GtACR1 blocking data and TrpA1 activation induced forgetting data shown above, indicate that *sickie* KD in the MP1 DAn impairs forgetting by reducing ongoing DAn activity.

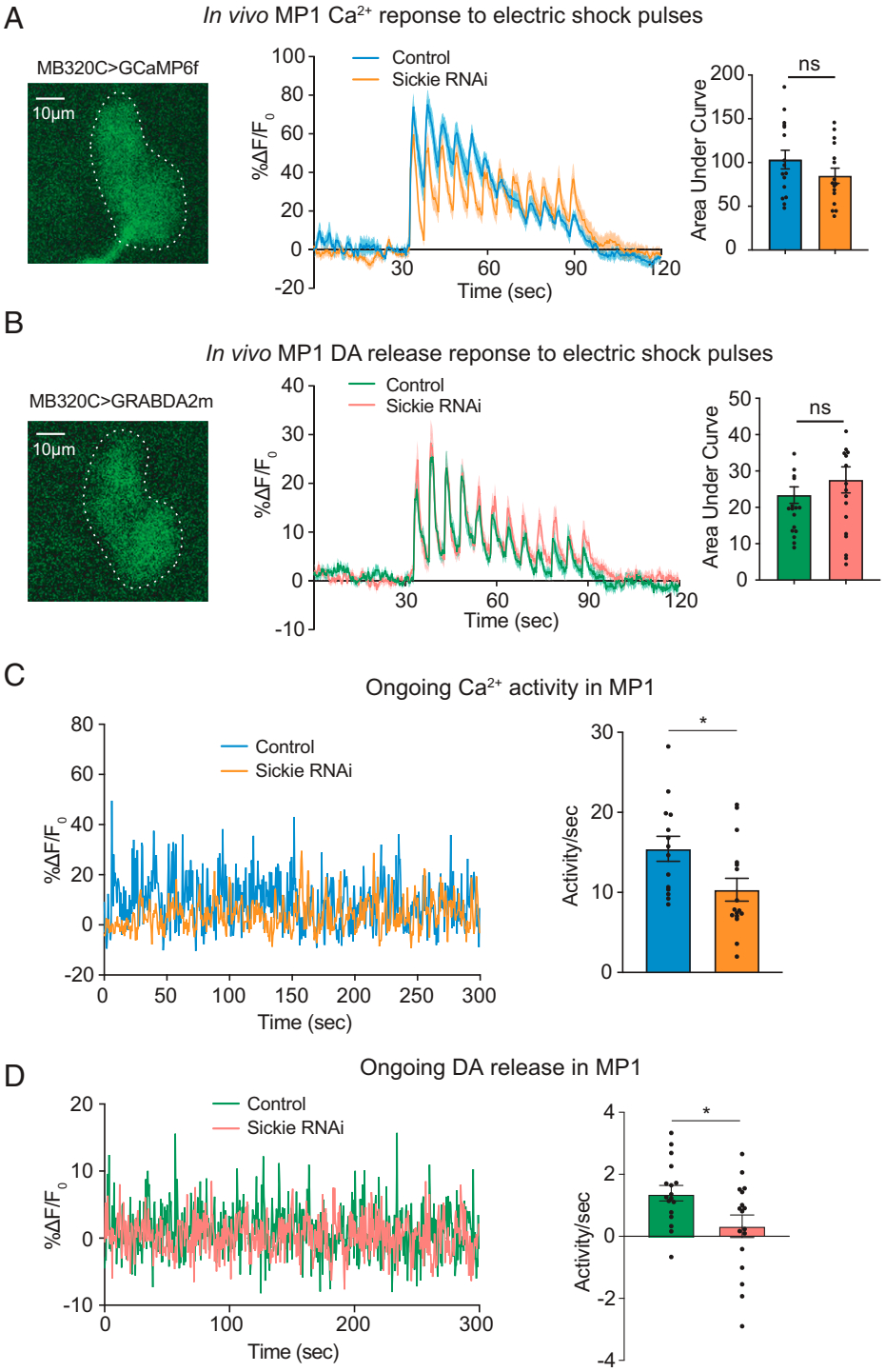

Fig. 4. *Sickie* KD in MP1 DAn reduces ongoing DAn activity. (*A*) *Sickie* KD in MP1 DAn did not significantly alter electric shock-induced calcium responses in the MP1 axon terminals (dotted outline, *Left*). Flies were subjected to 12 pulses of electric shock (90 V, 1.25 s every 5 s) between 30 and 90 s The mean response (*Center*) is shown as the dark lines and the SEM with lighter shading. The bar graph (*Right*) quantifies the electric shock response as the area under the curves between the two genotypes. Mann–Whitney *U* test; ns, not significant; $n = 16$; mean ± SEM. (*B*) *Sickie* KD in MP1 DAn did not significantly alter electric shock-induced DA release in the MP1 axon terminals (dotted outline, *Left*). Flies were subjected to 12 pulses of electric shock (90 V, 1.25 s every 5 s) between 30 and 90 s The mean response (*Center*) is shown as the dark lines and the SEM with lighter shading. The bar graph (*Right*) quantifies the electric shock response as the area under the curves between the two genotypes. Mann–Whitney *U* test, ns, not significant; $n = 16$; mean ± SEM. (*C*) *Sickie* KD in MP1 DAn decreased the ongoing Ca^{2+} activity in the MP1 region. (*Left*) Representative recordings using GCaMP6f. The bar graph (*Right*) quantifies the activity as the area under the curve between the two genotypes. Control: *MB320C*> +, *UAS-GCaMP6f*, *UAS-tdTomato*. *sickie* RNAi: *MB320C* > *sickie RNAi*^{54037}, *UAS-GCaMP6f*, *UAS-tdTomato*. Mann–Whitney *U* test, $*P < 0.05$; $n = 14$ to 16; mean ± SEM. (*D*) *Sickie* KD in MP1 DAn decreased the ongoing DA release in MP1. (*Left*) Representative recordings using GRAB-DA2m. The bar graph (*Right*) quantifies the activity as the area under the curve between the two genotypes. Control: *MB320C*> +, *UAS-GRABDA2m*, *UAS-tdTomato*. *sickie* RNAi: *MB320C* > *sickie RNAi*^{54037}, *UAS-GRABDA2m*, *UAS-tdTomato*. Mann–Whitney *U* test, $*P < 0.05$; $n = 17$; mean ± SEM.

No Detectable Differences in MP1 DAn Axonal Innervation and Connection to MBn between *sickie* KD and Control Flies. *Sickie* has been reported to regulate F-actin–mediated axon growth in the *Drosophila* MBn (16). This prompted the hypothesis that the reduction in ongoing DAn activity in *sickie* KD flies is due to a failure of MP1 DAn to innervate the MB neuropil correctly and to make the appropriate connections. We considered this hypothesis, despite our TARGET experiments (Fig. 1*G*) showing that *sickie* function is required in adult flies for forgetting, after the DAn extend their axonal projections (17, 27). To obtain additional data, we expressed a membrane-localized GFP in MP1 DAn. We did not detect any obvious morphological change of MP1 DAn projections to the MP1 region upon visual inspection of the confocal images, nor did we detect any difference in the GFP fluorescence of MP1 DAn projections (Fig. 5*A*). We also employed GRASP (GFP reconstitution across synaptic partners) (28, 29) to explore the integrity of synaptic connections between MP1 DAn axons and the MB neuropil. We again failed to find any obvious morphological change or significant difference in the GFP fluorescence intensity between control and *sickie* KD flies (Fig. 5*B*). Although we cannot rule out the possibility that subtle differences exist in these parameters between the two genotypes, the data indicate that there is no gross alteration in

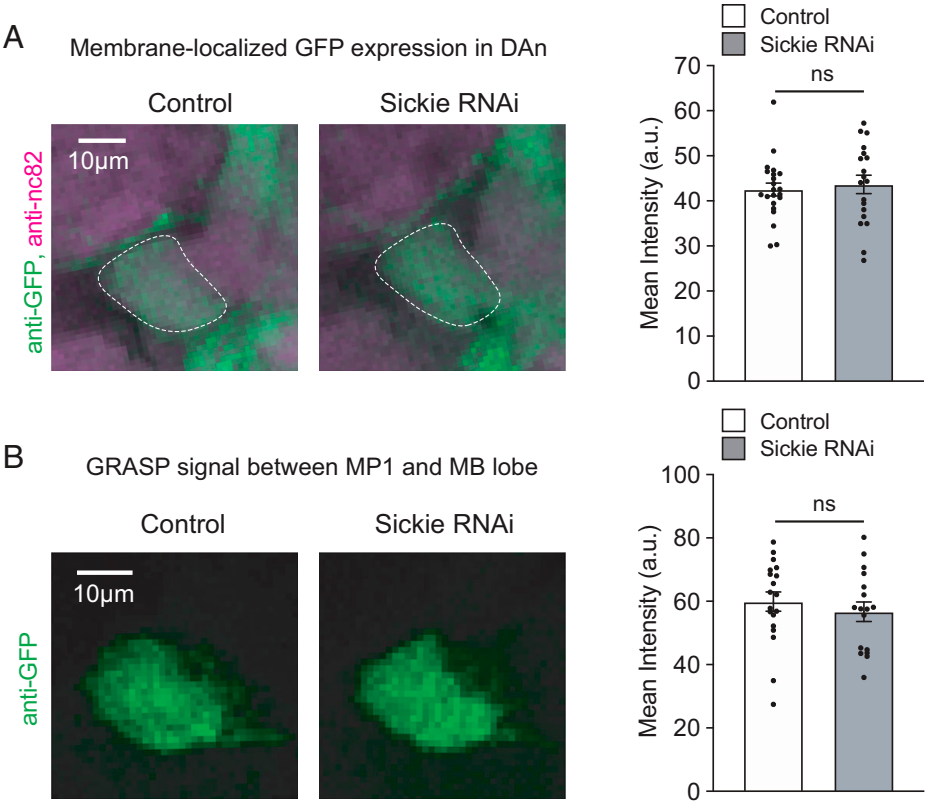

Fig. 5. No detectable differences in MP1 DAn axonal innervation and connection to MBn between *Sickie* KD and control flies. (*A*) *Sickie* KD in MP1 DAn did not alter the innervation of MP1 DAn in the MP1 region, visualized using membrane localized GFP. Quantitation of fluorescence intensity in the MP1 region is shown in the bar plot. Control: *TH-D′*, *tub-Gal80^{ts}*>+, *UAS-mCD8-GFP*. *sickie* RNAi: *TH-D′*, *tub-Gal80^{ts}* > *sickie RNAi^{54037}*, *UAS-mCD8-GFP*. Mann–Whitney *U* test, ns, not significant; n = 19 to 22; mean ± SEM. (*B*) The GRASP signal indicates that structural connections between MP1 DAn and MBn are not detectably altered by *sickie* KD in MP1 DAn. Quantitation of fluorescence intensity in the MP1 region is shown in the bar plot. Control: *MB* > *spGFP^{11}*, *MB320C*>+, *UAS-spGFP$^{1-10}$*. *sickie* RNAi: *MB* > *spGFP^{11}*, *MB320C* > *sickie RNAi^{54037}*, *UAS-spGFP$^{1-10}$*. Mann–Whitney *U* test, ns, not significant; n = 17 to 19; mean ± SEM.

axonal projections and connections in the *sickie* KD flies and are consistent with *sickie* KD altering some aspect of MP1 DAn function in adult flies.

Co-IP/MS Experiments Identify Sickie-Interacting Proteins. The failure to link *sickie's* role in forgetting through ongoing DAn activity with morphological changes prompted us to explore other possible mechanisms. Because little is known about Sickie's biochemical and physiological functions, we opted to collect unbiased knowledge of its involvement in molecular pathways and protein–protein interaction networks using co-IP/MS. We expressed a transgene encoding mCherry-tagged Sickie (mCherry-Sickie) to generate the bait for selecting interacting proteins and mCherry alone as control for co-IP/MS experiments. Magnetic beads preconjugated with mCherry antibody were used to enrich the mCherry-Sickie or mCherry proteins from whole head lysates (*nSyb-gal4*> *UAS-mCherry-sickie* or *UAS-mCherry*). After elution and in-gel digestion with trypsin, the samples were analyzed with liquid chromatography-tandem MS (LC-MS/MS). From three independent co-IP/MS experiments, a total of 1,206 proteins were detected with 2 or more unique peptides, 851 of which were unique to the mCherry-Sickie group (Fig. 6*A*). As expected, most of the proteins were found in this group with only 20 in the mCherry-only group.

After removing common contaminants found in MS experiments, we used the average of the total spectra count (TS) across the three experiments as one factor to select proteins with the highest likelihood of being authentic interactors. Since large proteins generally have a large TS, we introduced a normalization factor for size (protein coverage, PC), calculated as the ratio between TS and molecular mass (kDa), for each protein. The data analysis using these parameters (*Materials and Methods*) yielded a list of 215 proteins (including Sickie) as candidates with increased confidence (Fig. 6*B* and *SI Appendix*, Table S1). The 215 candidate proteins were analyzed for known or predicted interactions (STRING database), which identified "maintenance of presynaptic AZ structure" as the top biological process (gene ontology; including α-Spec, β-Spec, Brp, Synj, and RhoGAP100F from the 215 candidates) (Fig. 6*C*). Notably, three of these proteins (α-Spec, β-Spec, and Brp) were also among the top 10% MS candidates, selected by having PC and TS values in the top 10% for each parameter (Fig. 6*B*). Clustering of the 215 MS candidates using their protein–protein interaction scores from the STRING database also revealed protein clusters for vesicle trafficking and synaptic transmission (Fig. 6*D* and *SI Appendix*, Fig. S6). These results led to the hypothesis that Sickie might interact with presynaptic AZ components to regulate neurotransmitter release.

Sickie Physically and Genetically Interacts with Presynaptic AZ Protein Brp for Forgetting. We performed a focused RNAi behavioral screen for the protein candidates that had both PC and TS values within the top 10% for both parameters (α-Spec, Brp, β-Spec, ACC, Actn, GlyS, and Rab32) (Fig. 6*B*) to determine whether KD of any of these genes exhibit the same or opposite phenotype as *sickie* KD. This would offer evidence that they interact with *sickie* for forgetting. *Brp*, *α-Spec*, and *rab32* exhibited elevated performance in the initial test (*SI Appendix*, Fig. S7*A*). A rescreen with these three genes, each with its own paired control, showed that KD of *brp* in MP1 DAn (two independent RNAi), but not *α-Spec* or *rab32*, significantly increased 3-h memory (Fig. 7*A* and *SI Appendix*, Fig. S7 *B–D*). The memory-enhancement phenotype observed in *brp* KD group was not due to chromatin position effects (*SI Appendix*, Fig. S7 *C* and *E*). Given that Brp is one of the top candidates from the co-IP/MS results and KD of *brp* exhibited the same 3-h memory phenotype as *sickie* KD, these results suggested that Sickie may interact with Brp for forgetting.

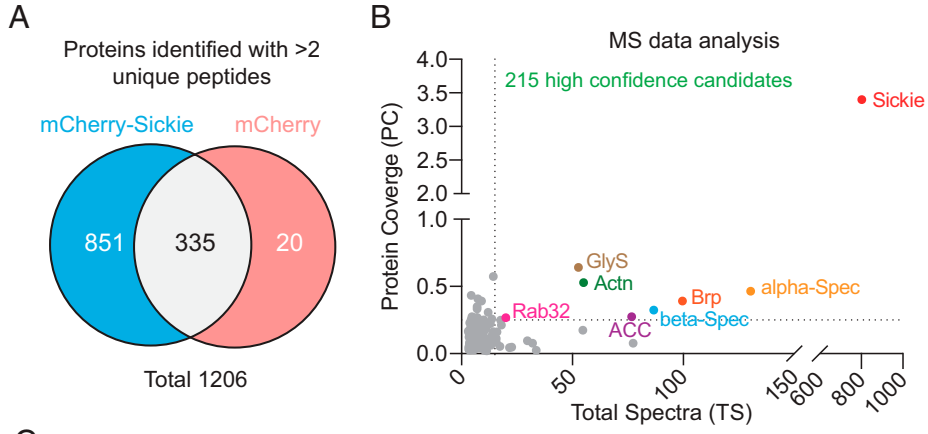

C

Top 5 biological process (Gene Ontology) associated with MS candidates

Biological process (Gene Ontology)	Strength	False discovery rate	Proteins related
Maintenance of presynaptic active zone structure	1.56	0.00058	alpha-Spec, beta-Spec, Brp, Synj, RhoGAP100F
Positive regulation of RNA splicing	1.45	0.0391	Hrb98DE, Hrb87F, Ps
Substrate adhesion-dependent cell spreading	1.42	0.0087	LanA, LanB1, LanB2, Tig
Striated muscle tissue development	1.42	0.0087	Flw, WupA, Fit1, LanB1
Non-associative learning	1.24	0.0205	Dnc, For, Me31B, Sgg

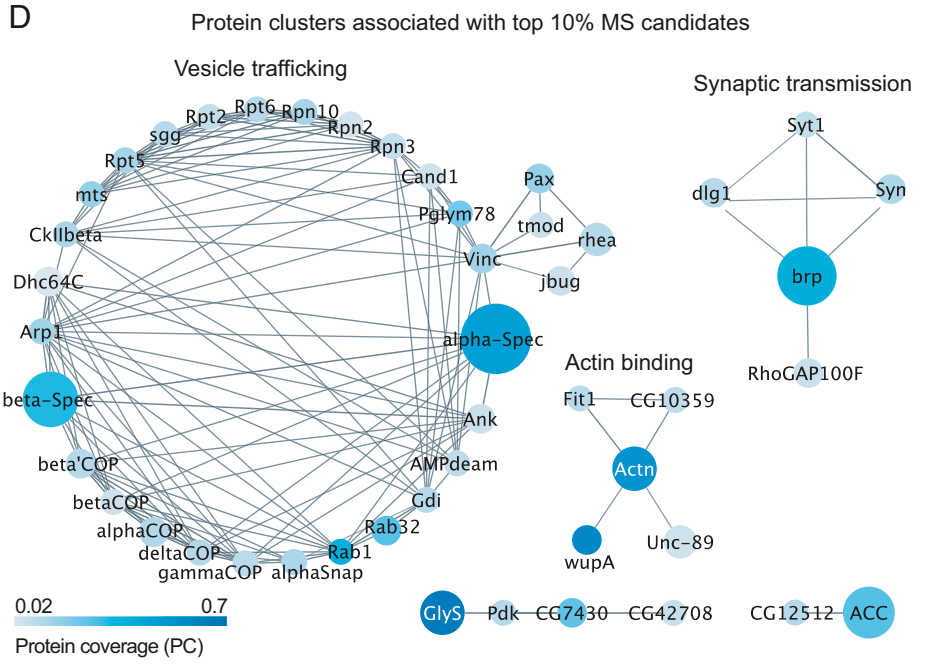

Fig. 6. Co-IP/MS to discover proteins interacting with Sickie. (*A*) Proteins with more than two unique peptides as detected with MS using either mCherry-Sickie or mCherry alone as bait. (*B*) Dot plot showing the average TS and PC for the 215 MS candidates (including Sickie). The dotted lines associated with each axis delimit (upper right quadrant) the proteins in the top 10% for both PC and TS. (*C*) Top five biological processes (gene ontology) associated with the 215 MS candidates predicted by the STRING database. "Strength" denotes the ratio between the number of proteins in the network that are annotated with a term and the number of proteins that the database expected to be annotated with this term in a random network of the same size. (*D*) Protein interaction networks associated with the top MS candidates. Markov clustering was performed with protein–protein interaction scores from the STRING database in Cytoscape. Node colors reflect the PC of the proteins; node sizes reflect the TS of the proteins. Gray lines between the nodes denote known or predicted protein–protein interactions (see *SI Appendix*, Fig. S6 for other identified protein networks).

Brp, the *Drosophila* ELKS/CAST/ERC homolog, is present in the AZ and required for the formation of T-bar, an electron-dense projection extending from the AZ plasma membrane into the presynaptic cytoplasm (30–32). Loss of *brp* function reduces the levels of Ca^{2+} channel subunit Cacophony (Cac) at the AZ and dramatically decreases evoked release at low stimulation frequencies (30). We reasoned that if Sickie interacts with Brp for normal Brp abundance and function, then *sickie* KD flies may exhibit a reduced Brp level and evoked release at low stimulation frequencies. If true, this would offer a mechanistic explanation for the reduction of ongoing Ca^{2+} activity and DA release for forgetting in *sickie* KD flies.

To test this hypothesis, we first confirmed the physical interaction between Sickie and Brp using co-IP and Western blotting experiments. We used antisera against mCherry to IP mCherry-Sickie and probed the IP for Brp. The results revealed that the anti-mCherry antisera immunopreciptated both mCherry-Sickie and Brp (Fig. 7*B* and *SI Appendix*, Fig. S8*A*). The reciprocal co-IP using Brp as bait also successfully pulled down mCherry-Sickie (Fig. 7*B* and *SI Appendix*, Fig. S8*B*). Together, these results demonstrate that Sickie can physically interact with Brp.

We next decided to study whether *sickie* KD alters Brp levels in MP1 DAn. To do this, we used a GFP labeled Brp construct (Brp-GFP) to estimate Brp levels in control and *sickie* KD flies. We found that *sickie* KD significantly reduced the level of Brp-GFP in the MP1 region (Fig. 7*C*). We also used the STaR method, which enabled epitope tagging of endogenously

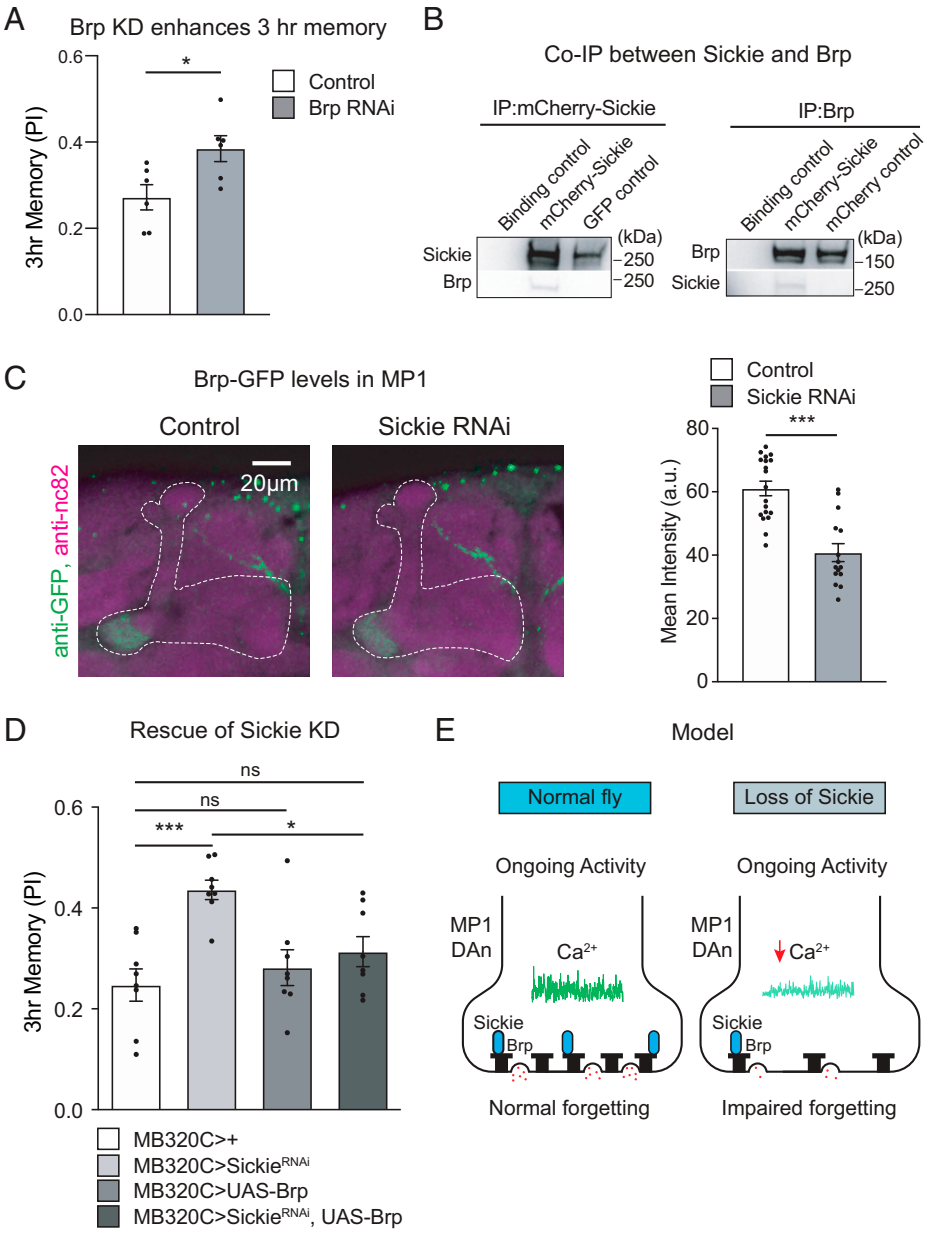

Fig. 7. Sickie physically and genetically interacts with the presynaptic AZ protein Brp for forgetting. (*A*) RNAi KD of *brp* in MP1 DAn increased 3-h memory. Control: *MB320C*>+. Brp RNAi: *MB320C* > *UAS-Brp*^{RNAi}. Student's *t* test, *$P < 0.05$; $n = 6$; mean ± SEM. (*B*) Representative immunoblots showing co-IP of Sickie and Brp. (*Left*) mCherry-Sickie as bait to pull down Brp-GFP. Flies expressing mCherry-Sickie and mCD8-GFP were used as a control for specificity, along with unconjugated binding control beads (Binding control). (*Right*) Brp used as bait to pull down mCherry-Sickie. Flies expressing mCherry were used as control along with beads coated with mouse IgG (binding control). $n = 3$ independent experiments. See full blots in *SI Appendix*, Fig. S8. (*C*) *Sickie* KD reduced Brp-GFP levels in the MP1 region as measured by immunohistochemistry. Quantitation of fluorescence in the MP1 region is shown in the bar plot. Control: *MB320C*>+, *UAS-Brp-GFP*. *sickie* RNAi: *MB320C* > *sickie RNAi*^{54037}, *UAS-Brp-GFP*. Mann–Whitney *U* test, ***$P < 0.001$; $n = 15$ to 19; mean ± SEM. (*D*) Overexpression of Brp (*UAS-brp*) in MP1 DAn rescued the forgetting phenotype observed in *sickie* KD flies. One-way ANOVA with Tukey's multiple comparisons. *$P < 0.05$, ***$P < 0.001$, ns, not significant; $n = 8$; mean ± SEM. (*E*) KD of *sickie* in MP1 DAn alters the abundance and/or function of the presynaptic AZ protein, Brp. Because Brp is an essential component of the T-bar in the presynaptic AZ, and it is required for the proper clustering of Ca^{2+} channels at the AZ, its reduction reduces the Ca^{2+} influx from ongoing activity and DA release from MP1 DAn. Since MP1 DAn bidirectionally regulates forgetting and reduced activity of MP1 DAn impairs forgetting, *sickie* KD reduces ongoing DAn activity producing an impairment of forgetting.

expressed Brp in an MP1 DAn-specific manner via flippase (FLP)/FRT recombination (33), along with brain expansion (34). Imaging of the MP1 region in the expanded brains revealed numerous Brp puncta, each identifying a putative AZ of MP1 DAn presynaptic terminals (*SI Appendix*, Fig. S9). Most importantly, we found that *sickie* KD significantly reduced the mean intensity and volume of Brp puncta, while increasing their number. Together, these data indicate that normal Sickie levels are required for the maturation and stability of Brp puncta at presynaptic terminals through physical interactions and when Sickie function is reduced, Brp puncta become fragmented.

These observations prompted the hypothesis that the reduced abundance of Brp in *sickie* KD flies causes the forgetting phenotype. If so, then restoring the level of Brp to at least control levels should rescue the *sickie* KD-induced forgetting phenotype. To test this, we overexpressed Brp (*UAS-brp*) in MP1 DAn and assayed whether it could rescue *sickie* KD-induced forgetting phenotype. Indeed, we found that overexpression of Brp in MP1 DAn fully rescued *sickie* KD-induced 3-h memory enhancement (Fig. 7*D*). In contrast, expression of a GFP construct (*UAS-mCD8-GFP*) along with the *sickie-RNAi* failed to rescue the *sickie* KD-induced 3-h memory enhancement (*SI Appendix*, Fig. S7*F*), arguing against *gal4* titration effects to explain the rescue by Brp overexpression. Taken together, these results indicate that Sickie physically and genetically interacts with Brp in MP1 DAn to regulate DA-based forgetting.

Discussion

Here, we present data showing that *sickie* function is required in a single DAn for the active forgetting of olfactory memory. It does this by regulating the ongoing release of DA, by interacting with and altering the function of the important presynaptic protein, Brp, in the maturation or stability of T-bars at presynaptic AZ. It is most interesting that of the dozen or more DAn that innervate the axons of the MBn in defined physical segments (17, 35), it is the MP1 DAn and its associated target—the heel of the MB neuropil (Fig. 1*E*)—that has the

most pronounced role in the process of active forgetting. This reinforces the conclusion that the 12 DAn in the PPL1 cluster have distinct and specialized functions. Supporting this conclusion, a prior study has shown that TrpA1 activation of MP1 DAn, but not other DAn in the PPL1 cluster, after training is sufficient to induce forgetting (3). Thus, the specific role for *sickie* in MP1 DAn for forgetting results from the intersection of *sickie*'s role in regulating ongoing DAn activity and the unique requirement of MP1 DAn for active forgetting. Most importantly, our results identify a player in the process of active forgetting and in the AZ protein machinery that regulates neurotransmitter release.

Our results also open the question about the developmental and physiological roles that have been described for *sickie*. *sickie* was previously reported to interact genetically with *rac1*, *slingshot*, and *cofilin* to regulate F-actin–mediated axon growth of *Drosophila* MBn (16). However, our behavioral data after temporal KD (Fig. 1*G*) and structural data (Fig. 5) argue against a similar developmental role for *sickie* in DAn, and point to an additional, physiological role in adult DAn after axon extension (17, 27). Nevertheless, it is intriguing that *sickie* genetically interacts with *rac1* and *cofilin* for developmental processes. These two genes are also involved in the MBn for active forgetting (1, 5, 6). Thus, the genes and their protein products can exhibit functional interactions that depend on cell type and developmental state. We did not observe Rac1, Slingshot, or Cofilin among the candidates from our co-IP/MS data, indicating that either Sickie has no direct physical interaction with these proteins in the adult head, or the interaction is too weak, sparse, or transient to be captured through antibody pulldowns.

However, it is possible that Sickie may mediate more subtle morphological changes in synapse structure. Indeed, we discovered putative physical interactors and protein clusters that point to possible roles in regulating fine synapse morphology. For example, the actin cross-linking protein Actn is among the top 10% of our MS candidates along with other cytoskeletal proteins like α- and β-Spec (Fig. 6 *B* and *D*). This observation suggests a role for Sickie in interacting with cytoskeletal proteins to control synapse structure. Our RNAi KD experiments of these cytoskeletal protein-encoding genes did not uncover a behavioral phenotype (*SI Appendix*, Fig. S7), but this could be due to lack of potency of the RNAi used for this focused screen.

Although we cannot rule out the possibility that *sickie* KD causes mild morphological changes of the DAn presynaptic terminals by interacting with cytoskeletal proteins to decrease the ongoing activity of the neuron (Fig. 4 *C* and *D*), our results point to altered DA release through Sickie's interaction with Brp. Brp was a top candidate from our co-IP/MS experiments (Fig. 6*B*); its KD in MP1 DAn produced the same elevated memory phenotype as *sickie* KD (Fig. 7*A* and *SI Appendix*, Fig. S7 *A*, *C*, and *D*). Brp abundance was reduced in *sickie* KD flies (Fig. 7*C* and *SI Appendix*, Fig. S9), and its overexpression rescued the forgetting phenotype of *sickie* KD (Fig. 7*D*). Brp is a component of the T-bar in the presynaptic AZ and is required for the proper clustering of Ca^{2+} channels at the AZ (30–32). It could be that the lack of proper clustering of the Ca^{2+} channels leads to the decrease in ongoing Ca^{2+} influx detected in MP1 DAn terminals (Fig. 4*C*). Complete loss-of-function of *brp* dramatically decreases the evoked release at low stimulation frequency, but does not abolish the release (30, 36), indicating that the protein participates in release but is not an absolute requirement. In a parallel way, *sickie* KD impairs ongoing DAn release but not electric shock-induced activity (Fig. 4 *B* and *D*). These observations align with one another, leading to the model that *sickie* KD reduces Brp abundance in MP1 DAn, reducing Ca^{2+} influx from ongoing activity, reducing DA release during ongoing activity, and impairing forgetting (Fig. 7*E*).

In addition to its role in Ca^{2+} channel clustering, Brp is required for the tethering of synaptic vesicles in the AZ cytomatrix via its C-terminal sequence at the neuromuscular junction of *Drosophila* larvae (37, 38), potentially through its genetic interaction with the SNARE regulator, Complexin (39). Our protein network and gene ontology analysis also uncovered a protein cluster for synaptic transmission involving Brp, Syt1, Syn, Dlg1, and RhoGAP100F (Fig. 6*D*). Syt1 is a synaptic vesicle protein that is essential for Ca^{2+}-dependent release (40, 41), whereas Syn functions for synaptic vesicle clustering and synaptic transmission (42, 43). Thus, our studies may also suggest a role for Sickie in synaptic vesicle trafficking and tethering for neurotransmitter release, either by interacting with Brp or other proteins. Because of the highly conserved structure of the presynaptic AZ and neurotransmitter release machinery across species, our findings suggest a possible but unexplored role for *sickie's* homologs in neurotransmitter release and forgetting in other species.

Materials and Methods

Fly Husbandry and Strains. Fly stocks were cultured on standard *Drosophila* food at 23 °C. Experimental crosses were maintained at 25 °C unless otherwise stated, with 70% relative humidity and a 12/12-h, light/dark cycle. Flies of both sexes were used unless otherwise stated.

The Gal4 lines used in this study include: *TH-Gal4* (8848, Bloomington *Drosophila* Stock Center; BDSC), *c150-Gal4* (44), *c061-Gal4* (30845, BDSC), *MZ604-Gal4* (45), *NP2755-Gal4* (45), *MZ840-Gal4* (45), *NP7198-Gal4* (45), *NP7135-Gal4* (45), *MB304B-Split Gal4* (35), *MB065B-Split Gal4* (35), *MB320C-Split Gal4* (46), *TH-D'* (47), and *nSyb-Gal4* (gift from Julie Simpson, Santa Barbara, California, USA).

The *UAS-RNAi* fly lines used in this study were either from the KK RNAi library (Vienna *Drosophila* Resource Center, VDRC) or Harvard Transgenic RNAi Project (TRiP) RNAi library (available from BDSC). *UAS-RNAi* fly lines from the KK RNAi library include: control line (60100, VDRC), *UAS-sickie^{RNAi}* (107037, VDRC), and *UAS-brp^{RNAi}* (104630, VDRC). *UAS-RNAi* fly lines from the Harvard TRiP RNAi library include: control lines (36303 or 36304, BDSC), *UAS-sickie^{RNAi}* (54037, 53315, BDSC), *UAS-brp^{RNAi}* (25891, BDSC), *UAS-rab32^{RNAi}* (28002, BDSC), *UAS-Gly^{RNAi}* (34930, BDSC), *UAS-alpha-Spec^{RNAi}* (31209, BDSC), *UAS-beta-Spec^{RNAi}* (42802, BDSC), *UAS-ACC^{RNAi}* (34885), *UAS-Actn^{RNAi}* (34874, BDSC). Additional UAS lines employed include: *UAS-Dcr2* (60008, 60009, VDRC), *UAS-sickie* (16), *UAS-mCherry-sickie* (16), *UAS-mCD8-GFP* (48), *UAS-GCaMP6f* (42747, BDSC), *UAS-myr-tdTomato* (32221, BDSC), *UAS-GRABDA2m* (49), *UAS-GtACR1* (26) (gift from Michael Nitabach, New Haven, Connecticut, USA), *UAS-TNT* (28838, BDSC), *UAS-TrpA1* (50), *UAS-Brp-GFP* (gift from Stephan Sigrist), *UAS-Brp* (gift from Stephan Sigrist, Berlin, Germany), STaR [UAS-FLP, brp(FRT.Stop)V5-2A-LexA-VP16, 55751, BDSC], *UAS-mCherry* (35787, BDSC), *tub-Gal80^{ts}* (18), *MB-spGFP^{11}* (51), and *UAS-spGFP$^{1-10}$* (28).

A detailed description of experimental methods can be found in the *SI Appendix*.

Data, Materials, and Software Availability. The MS raw data have been deposited at MassIVE repository, https://massive.ucsd.edu/ProteoSAFe/static/massive.jsp (accession no. MSV000090127) (52). All other data are included in the main text and *SI Appendix*.

ACKNOWLEDGMENTS. We thank Dr. Stephan Sigrist for providing the *UAS-Brp-GFP* and *UAS-Brp* fly lines; Dr. Michael N. Nitabach and Dr. Adam Claridge-Chang for providing the *UAS-GtACR1* fly line; Dr. Yulong Li for providing the *UAS-GRABDA2m* fly line; the Janelia Research Campus for providing the split *gal4* lines; Gogce C. Crynen for helpful discussions and advice about mass spectrometry data analysis; and Erica Walkinshaw for expert technical support. This work was supported by Grants R35NS097224 and R37NS19904.

1. R. L. Davis, Y. Zhong, The biology of forgetting–A perspective. *Neuron* **95**, 490–503 (2017).
2. T. J. Ryan, P. W. Frankland, Forgetting as a form of adaptive engram cell plasticity. *Nat. Rev. Neurosci.* **23**, 173–186 (2022).
3. J. A. Berry, I. Cervantes-Sandoval, E. P. Nicholas, R. L. Davis, Dopamine is required for learning and forgetting in *Drosophila*. *Neuron* **74**, 530–542 (2012).
4. J. A. Berry, I. Cervantes-Sandoval, M. Chakraborty, R. L. Davis, Sleep facilitates memory by blocking dopamine neuron-mediated forgetting. *Cell* **161**, 1656–1667 (2015).
5. Y. Shuai *et al.*, Forgetting is regulated through Rac activity in *Drosophila*. *Cell* **140**, 579–589 (2010).
6. I. Cervantes-Sandoval, M. Chakraborty, C. MacMullen, R. L. Davis, Scribble scaffolds a signalosome for active forgetting. *Neuron* **90**, 1230–1242 (2016).
7. J. M. Sabandal, J. A. Berry, R. L. Davis, Dopamine-based mechanism for transient forgetting. *Nature* **591**, 426–430 (2021).
8. E. Walkinshaw *et al.*, Identification of genes that promote or inhibit olfactory memory formation in *Drosophila*. *Genetics* **199**, 1173–1182 (2015).
9. E. Foley, P. H. O'Farrell, Functional dissection of an innate immune response by a genome-wide RNAi screen. *PLoS Biol.* **2**, E203 (2004).
10. E. Stringham, N. Pujol, J. Vandekerckhove, T. Bogaert, unc-53 controls longitudinal migration in C. elegans. *Development* **129**, 3367–3379 (2002).
11. T. Maes, A. Barceló, C. Buesa, Neuron navigator: A human gene family with homology to unc-53, a cell guidance gene from Caenorhabditis elegans. *Genomics* **80**, 21–30 (2002).
12. K. L. Schmidt *et al.*, The cell migration molecule UNC-53/NAV2 is linked to the ARP2/3 complex by ABI-1. *Development* **136**, 563–574 (2009).
13. F. Tan *et al.*, Neuron navigator 2 overexpression indicates poor prognosis of colorectal cancer and promotes invasion through the SSH1L/cofilin-1 pathway. *J. Exp. Clin. Cancer Res.* **34**, 117 (2015).
14. B. Davidson *et al.*, Neuron navigator-2 and cyclin D2 are new candidate prognostic markers in uterine sarcoma. *Virchows Arch.* **471**, 355–362 (2017).
15. W. Hu *et al.*, NAV2 facilitates invasion of cutaneous melanoma cells by targeting SNAI2 through the GSK-3β/β-catenin pathway. *Arch. Dermatol. Res.* **311**, 399–410 (2019).
16. T. Abe *et al.*, The NAV2 homolog Sickie regulates F-actin-mediated axonal growth in *Drosophila* mushroom body neurons via the non-canonical Rac-Cofilin pathway. *Development* **141**, 4716–4728 (2014).
17. Z. Mao, R. L. Davis, Eight different types of dopaminergic neurons innervate the *Drosophila* mushroom body neuropil: Anatomical and physiological heterogeneity. *Front. Neural Circuits* **3**, 5 (2009).
18. S. E. McGuire, P. T. Le, A. J. Osborn, K. Matsumoto, R. L. Davis, Spatiotemporal rescue of memory dysfunction in *Drosophila*. *Science* **302**, 1765–1768 (2003).
19. M. Schwaerzel *et al.*, Dopamine and octopamine differentiate between aversive and appetitive olfactory memories in *Drosophila*. *J. Neurosci.* **23**, 10495–10502 (2003).
20. P.-Y. Y. Plaçais *et al.*, Slow oscillations in two pairs of dopaminergic neurons gate long-term memory formation in *Drosophila*. *Nat. Neurosci.* **15**, 592–599 (2012).
21. S. Himmelreich *et al.*, Dopamine receptor damb signals via gq to mediate forgetting in *Drosophila*. *Cell Rep.* **21**, 2074–2081 (2017).
22. J. A. Berry, A. Phan, R. L. Davis, Dopamine neurons mediate learning and forgetting through bidirectional modulation of a memory trace. *Cell Rep.* **25**, 651–662.e5 (2018).
23. Y. Aso *et al.*, Specific dopaminergic neurons for the formation of labile aversive memory. *Curr. Biol.* **20**, 1445–1451 (2010).
24. Y. Aso *et al.*, Three dopamine pathways induce aversive odor memories with different stability. *PLoS Genet.* **8**, e1002768 (2012).
25. T. Tully, T. Preat, S. C. Boynton, M. Del Vecchio, Genetic dissection of consolidated memory in *Drosophila*. *Cell* **79**, 35–47 (1994).
26. F. Mohammad *et al.*, Optogenetic inhibition of behavior with anion channelrhodopsins. *Nat. Methods* **14**, 271–274 (2017).
27. V. Hartenstein, L. Cruz, J. K. Lovick, M. Guo, Developmental analysis of the dopamine-containing neurons of the *Drosophila* brain. *J. Comp. Neurol.* **525**, 363–379 (2017).
28. E. H. Feinberg *et al.*, GFP reconstitution across synaptic partners (GRASP) defines cell contacts and synapses in living nervous systems. *Neuron* **57**, 353–363 (2008).
29. M. D. Gordon, K. Scott, Motor control in a *Drosophila* taste circuit. *Neuron* **61**, 373–384 (2009).
30. R. J. Kittel *et al.*, Bruchpilot promotes active zone assembly, Ca2+ channel clustering, and vesicle release. *Science* **312**, 1051–1054 (2006).
31. D. A. Wagh *et al.*, Bruchpilot, a protein with homology to ELKS/CAST, is required for structural integrity and function of synaptic active zones in *Drosophila*. *Neuron* **49**, 833–844 (2006).
32. W. Fouquet *et al.*, Maturation of active zone assembly by *Drosophila* Bruchpilot. *J. Cell Biol.* **186**, 129–145 (2009).
33. Y. Chen *et al.*, Cell-type-specific labeling of synapses in vivo through synaptic tagging with recombination. *Neuron* **81**, 280–293 (2014).
34. S. M. Asano *et al.*, Expansion microscopy: Protocols for imaging proteins and RNA in cells and tissues. *Curr. Protoc. Cell Biol.* **80**, e56 (2018).
35. Y. Aso *et al.*, The neuronal architecture of the mushroom body provides a logic for associative learning. *eLife* **3**, e04577 (2014).
36. T. C. Südhof, The presynaptic active zone. *Neuron* **75**, 11–25 (2012).
37. S. Hallermann *et al.*, Naked dense bodies provoke depression. *J. Neurosci.* **30**, 14340–14345 (2010).
38. T. Matkovic *et al.*, The Bruchpilot cytomatrix determines the size of the readily releasable pool of synaptic vesicles. *J. Cell Biol.* **202**, 667–683 (2013).
39. N. Scholz *et al.*, Complexin cooperates with Bruchpilot to tether synaptic vesicles to the active zone cytomatrix. *J. Cell Biol.* **218**, 1011–1026 (2019).
40. R. Fernández-Chacón *et al.*, Synaptotagmin I functions as a calcium regulator of release probability. *Nature* **410**, 41–49 (2001).
41. T. C. Südhof, Calcium control of neurotransmitter release. *Cold Spring Harb. Perspect. Biol.* **4**, a011353 (2012).
42. T. W. Rosahl *et al.*, Essential functions of synapsins I and II in synaptic vesicle regulation. *Nature* **375**, 488–493 (1995).
43. P. Greengard, F. Valtorta, A. J. Czernik, F. Benfenati, Synaptic vesicle phosphoproteins and regulation of synaptic function. *Science* **259**, 780–785 (1993).
44. J. Dubnau *et al.*, The staufen/pumilio pathway is involved in *Drosophila* long-term memory. *Curr. Biol.* **13**, 286–296 (2003).
45. N. K. Tanaka, H. Tanimoto, K. Ito, Neuronal assemblies of the *Drosophila* mushroom body. *J. Comp. Neurol.* **508**, 711–755 (2008).
46. T. Hige, Y. Aso, M. N. Modi, G. M. Rubin, G. C. Turner, Heterosynaptic plasticity underlies aversive olfactory learning in *Drosophila*. *Neuron* **88**, 985–998 (2015).
47. Q. Liu, S. Liu, L. Kodama, M. R. Driscoll, M. N. Wu, Two dopaminergic neurons signal to the dorsal fan-shaped body to promote wakefulness in *Drosophila*. *Curr. Biol.* **22**, 2114–2123 (2012).
48. T. Lee, L. Luo, Mosaic analysis with a repressible cell marker for studies of gene function in neuronal morphogenesis. *Neuron* **22**, 451–461 (1999).
49. F. Sun *et al.*, Next-generation GRAB sensors for monitoring dopaminergic activity in vivo. *Nat. Methods* **17**, 1156–1166 (2020).
50. F. N. Hamada *et al.*, An internal thermal sensor controlling temperature preference in *Drosophila*. *Nature* **454**, 217–220 (2008).
51. U. Pech, A. Pooryasin, S. Birman, A. Fiala, Localization of the contacts between Kenyon cells and aminergic neurons in the *Drosophila* melanogaster brain using SplitGFP reconstitution. *J. Comp. Neurol.* **521**, 3992–4026 (2013).
52. R. Davis, Active forgetting requires Sickie function in a dedicated dopamine circuit in Drosophila. MassIVE repository. https://massive.ucsd.edu/ProteoSAFe/dataset.jsp?task=6d198e3661eb4a69b331826146e01ed3. Accessed 6 September 2022.